A Vortex-Force Formalization Implementation for Representing Wave Effects on Currents

COMPAS -SWAN unstructured coupled modelling suite

Cagil Kirezci, Mike Herzfeld, Farhan Rizwi, Vanessa Hernaman, Ron Hoeke

Environment, CSIRO, Australia

Australia's National Science Agency

11/04/2024

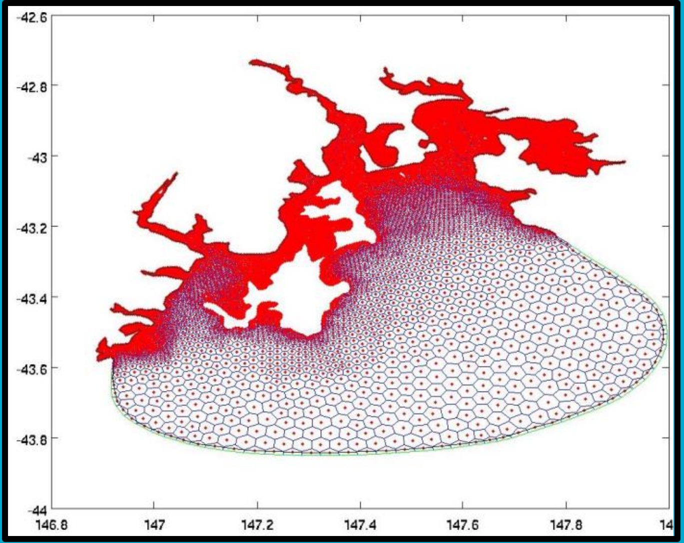

Wave-Flow Coupling –Nearshore Application

"Surface waves affect the upper-ocean circulation, air–sea fluxes, and cross-shelf exchange due to both conservative and non-conservative effects." (Romero et al., 2020)

WEC terms can impact;

- Addition of waves can impact elevation level
- Influence hydro-sedimentary dynamics in the coastal zone
- Contribute to storm surge, extreme water levels
- Wave impacts on currents & currents influence on waves

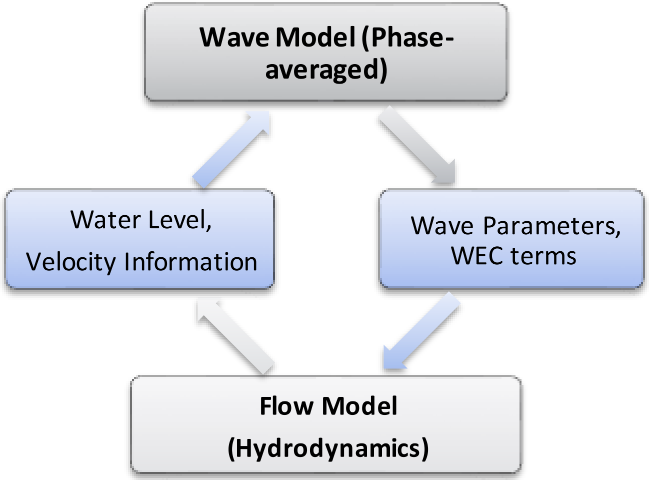

Wave-Flow Coupling –Nearshore Application

The coupling of these wave-current interactions is achieved by averaging the rapidly oscillating surface waves over long time-scales to deliver what is known as the Wave Effect on Currents (WEC).

Nearshore application with unstructured grid;

- Increased CFL conditions
- Spurious increases
- Non-conservative wave processes

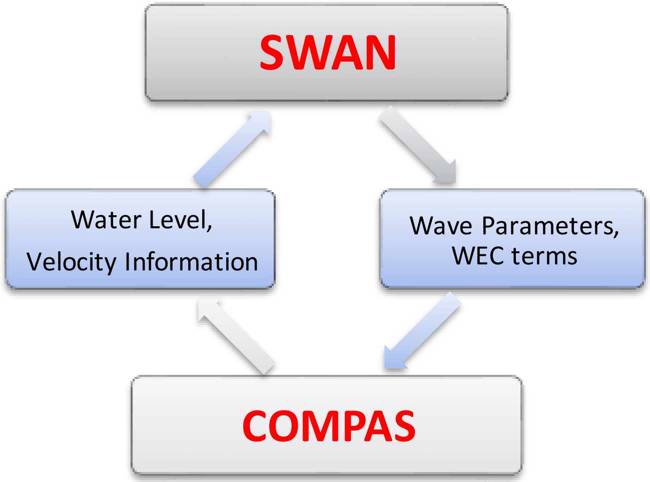

COMPAS- SWAN Coupling

Evaluate and develop next-generation numerical modelling techniques and tools for incorporation, with the aim of improved prediction of littoral dynamics at a greater range of spatial scales

The models: COMPAS & SWAN

❖ **COMPAS (Coastal Ocean Marine Prediction Across Scales)** - 3D finite volume unstructured hydrodynamic model in CSIRO's Environmental Modelling System (EMS). (Herzfeld,2006; Herzfeld et al.,2020)

- Used at scales ranging from estuaries to regional ocean domains
- COMPAS uses an orthogonal centroidal Voronoi tessellation on arbitrary polygons. The triangle created from joining cell centres surrounding a given vertex is the Delaunay dual is a Voronoi diagrams are the dual of a Delaunay triangulation
- Operates on Arakawa C-grid, whereby normal velocity components are staggered at the edges of Voronoi cells, with fluid height and tracer variables located at cell centres (Herzfeld et.al., 2020)
- **Advantages of hexagonal mesh:**

-spurious modes associated with triangular C-grid meshes are absent in these hexagonal cases.

- works well with finite-volume models

❖ **SWAN (Simulating Waves Nearshore)** (Booij et al., 1999; Zijlema et al., 2010) 3^{rd} gen phase averaged wave model

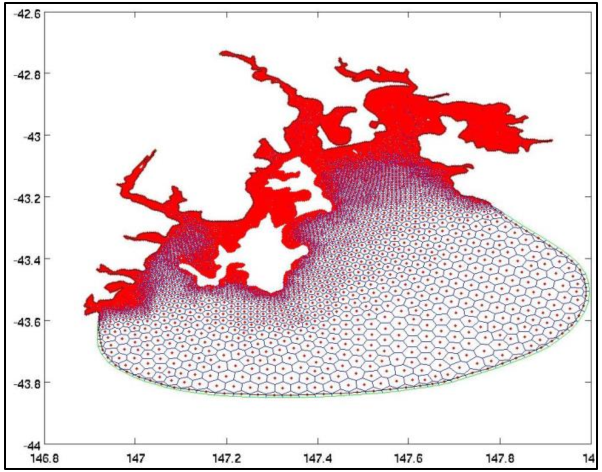

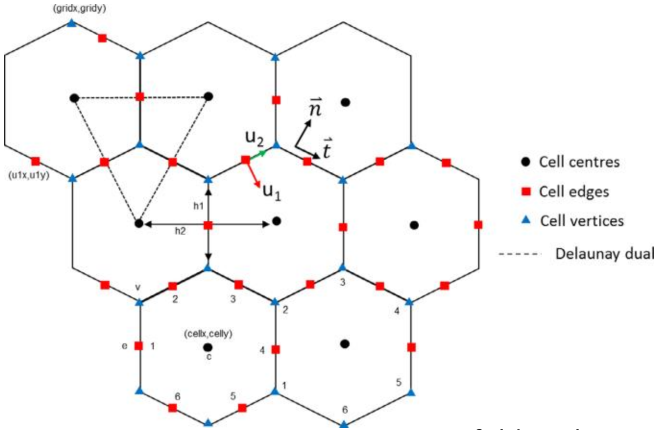

Figure: Herzfeld et.al., 2020

Mesh Generation

- JIGSAW (Engwirda, 2017) designed for TRiSK FV scheme Delaunay triangulation - Centroidal Voronoi Tessellation
- The horizontal mesh must be an orthogonal, centroidal and well-centred ‘primal-dual’ tessellation, typically consisting of collections of Voronoi cells and their dual Delaunay triangles.

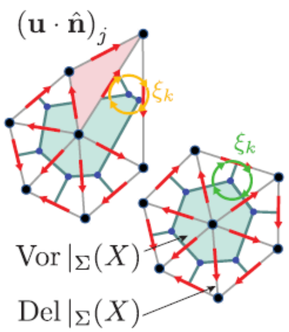

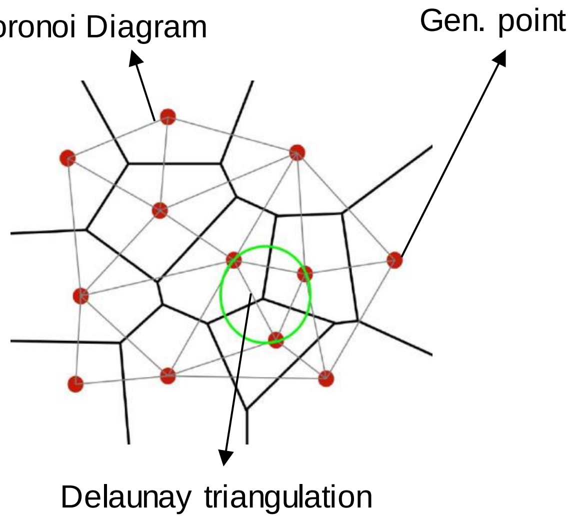

Figure:Herzfeld, 2018

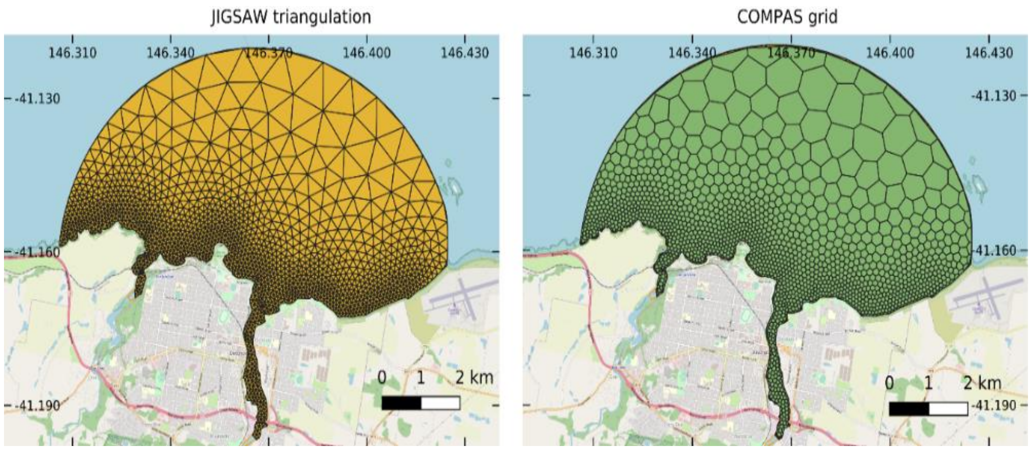

Figure: Farhan Rizwi

Vortex- Force Formalization and Why?

- Eulerian Framework (Quasi- Eulerian)
- Vortex-force representation decomposes the main wave-averaged effects into physically understandable concepts of vortex force, Bernoulli head, and nonconservative processes
  - explicit inclusion of different type of wave–current interaction
  - incorporate impacts of depth-limited wave dissipation terms (e.g. wave breaking), higher order nonlinear wave impacts.
  - Vertical components of the 3d Radiation stress tensors wave radiation stress change very fast with depth
- Uchiyama et al., (2010) and Kumar et al., (2012) extended McWilliams et al. (2004) to consider non-conservative conditions by adding breaking waves, roller waves, bottom and surface streaming and wave-enhanced mixing through empirical formulas. (ROMS, COAWST, SCHISM)

*Bernoulli Head**

*Nonconservative WEC terms**

Momentum

$$\frac{\partial \mathbf{u}}{\partial t} + (\mathbf{u}\cdot\nabla_\perp)\mathbf{u} + w\frac{\partial \mathbf{u}}{\partial z} + f\hat{\mathbf{z}}\times\mathbf{u} + \nabla_\perp\phi - \mathbf{F} = -\nabla_\perp \mathcal{K} + \mathbf{J} + \mathbf{F}^w$$

Surface Streaming — Whitecapping Disp.* — Wave Roller

$$\mathbf{F}^w(\mathcal{F}^{w\xi}, \mathcal{F}^{w\eta}) = \mathbf{B}^{bf} + \mathbf{B}^{sf} + \mathbf{B}^{wb} = \mathbf{B}^{bf} + \mathbf{B}^{sf} + \mathbf{B}^{wcap} + \mathbf{B}^{b} + \mathbf{B}^{r}$$

Bottom Dissipation* — Wave Breaking* — Depth-Limited wave Breaking*

*Conservative Vortex Force**

$$\mathbf{J} = -\hat{\mathbf{z}}\times\mathbf{u}^{St}((\hat{\mathbf{z}}\cdot\nabla_\perp\times\mathbf{u})+f) - w^{St}\frac{\partial \mathbf{u}}{\partial z},$$

Continuity

$$\frac{\partial p}{\partial z} + \frac{g\rho}{\rho_o} = -\frac{\partial \mathcal{K}}{\partial z} + u_s\cdot\frac{\partial u}{\partial z}$$

*Stokes Drift**

Transport

$$\frac{\partial c}{\partial t} + (\mathbf{u}\cdot\nabla_\perp)c + w\frac{\partial c}{\partial z} - \mathcal{C} = -(\mathbf{u}^{St}\cdot\nabla_\perp)c - w^{St}\frac{\partial c}{\partial z} + \frac{1}{2}\frac{\partial}{\partial z}\left[\mathcal{E}\frac{\partial c}{\partial z}\right]$$

*calculated in SWAN

COMPAS-SWAN Coupling Technical

- No model coupler
- Compile SWAN as a library object to which COMPAS can link using C interoperability protocols
- During initialisation within SWAN, pointers to variables within this data structure are set up.
- COMPAS initialises and manages memory for wave variables
- SWAN updates information for those variables by writing directly to the memory addressed rather than transferring the actual data

Variable	Description	Method
COMPAS STE	Stokes Drift	Romero et al. (2021)
COMPAS K	Effective Wavenumber	Romero et al. (2021)
COMPAS KB	Bernoulli Head (Wave-Induced Pressure)	WW3, Bennis et al. (2011)
COMPAS FWCAP	Whitecapping	SWAN + Uchiyama et al. (2010)
COMPAS FBRE	Depth-induced wave breaking	SWAN + Uchiyama et al. (2010)
COMPAS FBOT	Bottom Friction Dissipation	SWAN + Uchiyama et al. (2010)
COMPAS FSUR	Surface Streaming	SWAN + Kumar et al. (2012)
COMPAS FROL	Surface Roller Dissipation	Svendsen(1984) + Kumar et al. (2012)

Testbed region: Mandurah, Western Australia

- Geographical Features

- The nearshore reefs
- Tidal channels
- Estuary
- Leeuwin Current

-Observation Points

in-situ coastal wave and circulation observations are available in this region

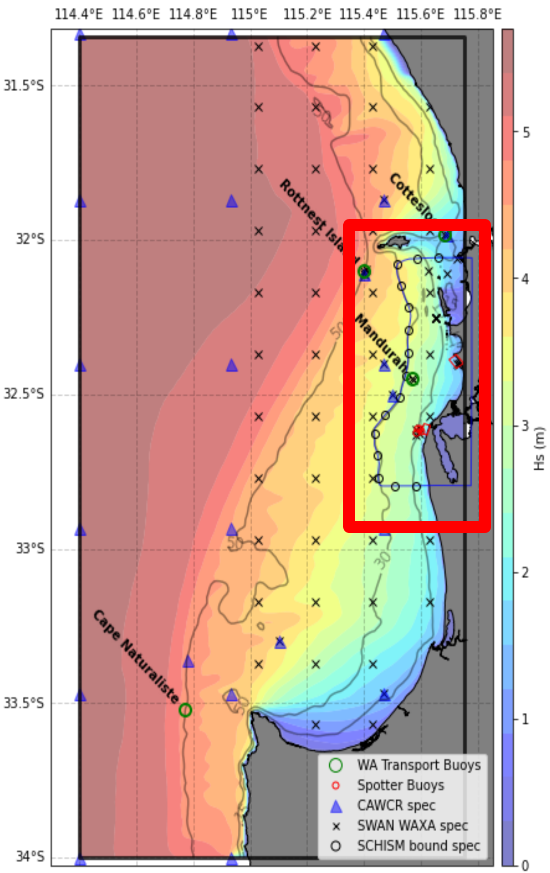

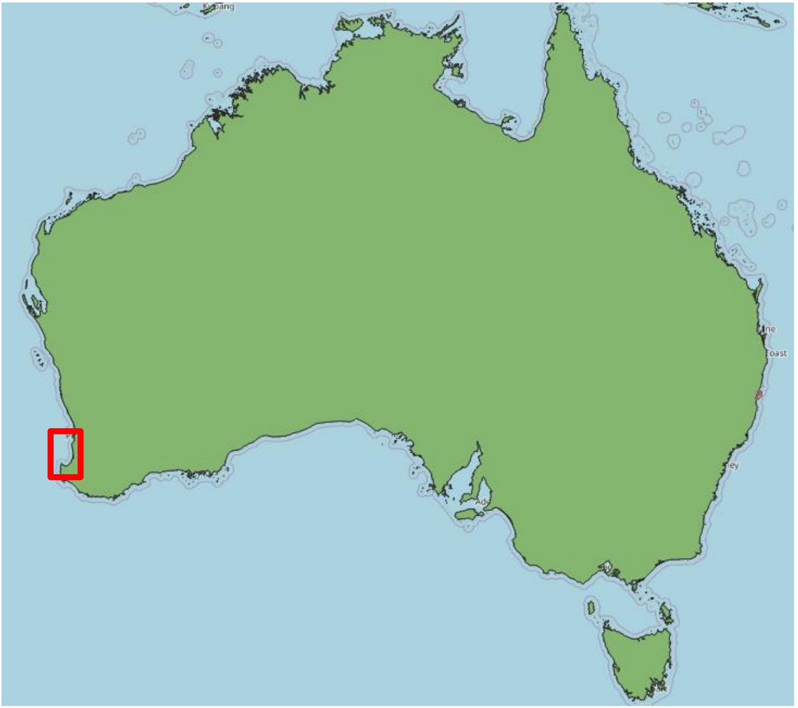

Testbed region: Mandurah, Western Australia

- Geographical Features

- The nearshore reefs
- Tidal channels
- Estuary
- Leeuwin Current

-Observation Points

in-situ coastal wave and circulation observations are available in this region

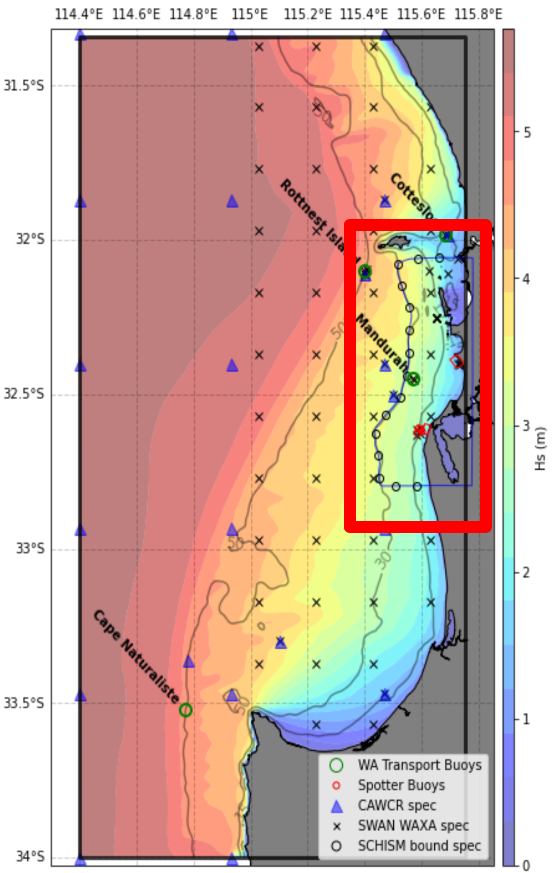

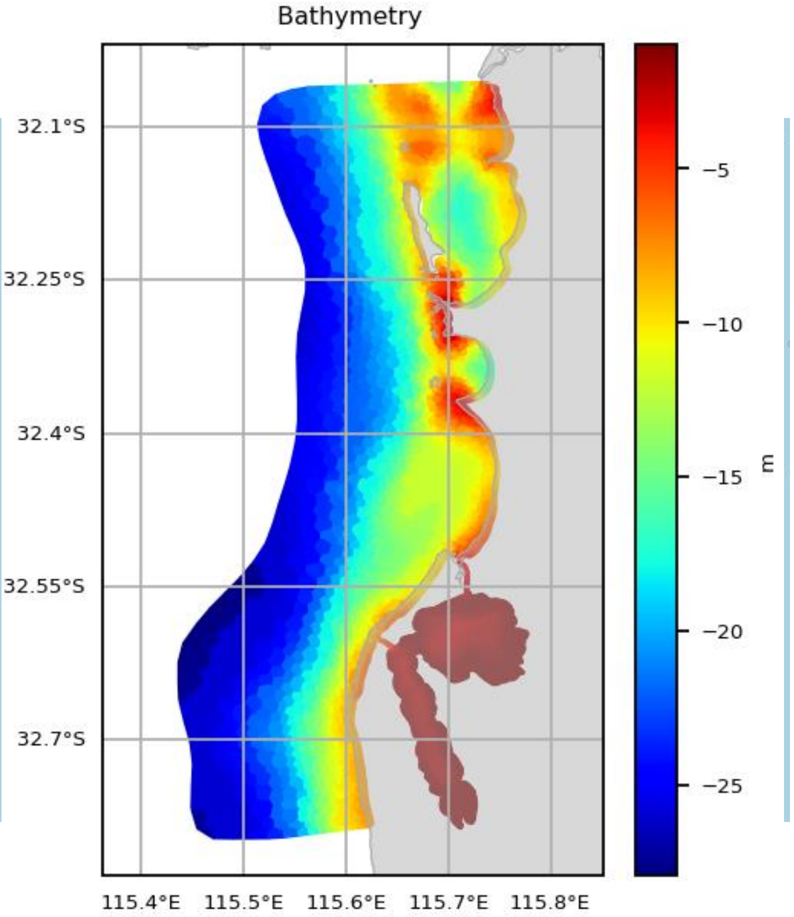

Mandurah Testbed : June 2019- August 21

Resolution

- 100 m resolution at the coast
- 3000 m at the open boundary
- ~40000 indices
- SWAN t=15 min , COMPAS t=10 sec

Forcing Fields

- **Winds**

  ACCESS Winds -12.5 km (G)

- **Wave Forcing**

  Regional SWAN hindcast (500m) downscaled from Auswave G3 Operational Wave Model (WW3) , Zieger and Greenslade (2021)

- **Water Level**

  BRAN2020 OFAM3 (MOM5) (0.1 degree)

  Chamberlain et al. (2021)

- **Tides**

  TPXO Tides

  Egbert, G.D. and Svetlana Y.E (2002)

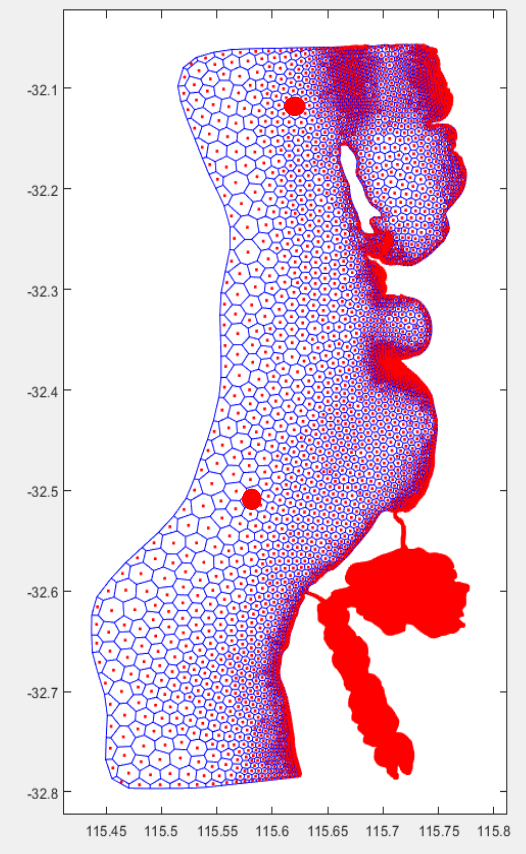

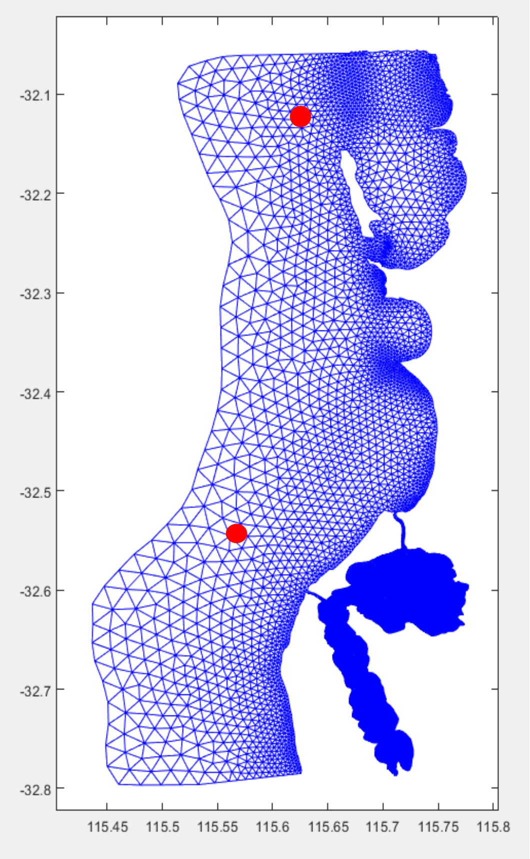

Manduraḥ Testbed : June 2019- August 21

Resolution

- 100 m resolution at the coast
- 3000 m at the open boundary
- ~40000 indices
- SWAN t=15 min , COMPAS t=10 sec

Forcing Fields

- **Winds**

  ACCESS Winds -12.5 km (G)

- **Wave Forcing**

  Regional SWAN hindcast (500m) downscaled from Auswave G3 Operational Wave Model (WW3) , Zieger and Greenslade (2021)

- **Water Level**

  BRAN2020 OFAM3 (MOM5) (0.1 degree)
  Chamberlain et al. (2021)

- **Tides**

  TPXO Tides
  Egbert, G.D. and Svetlana Y.E (2002)

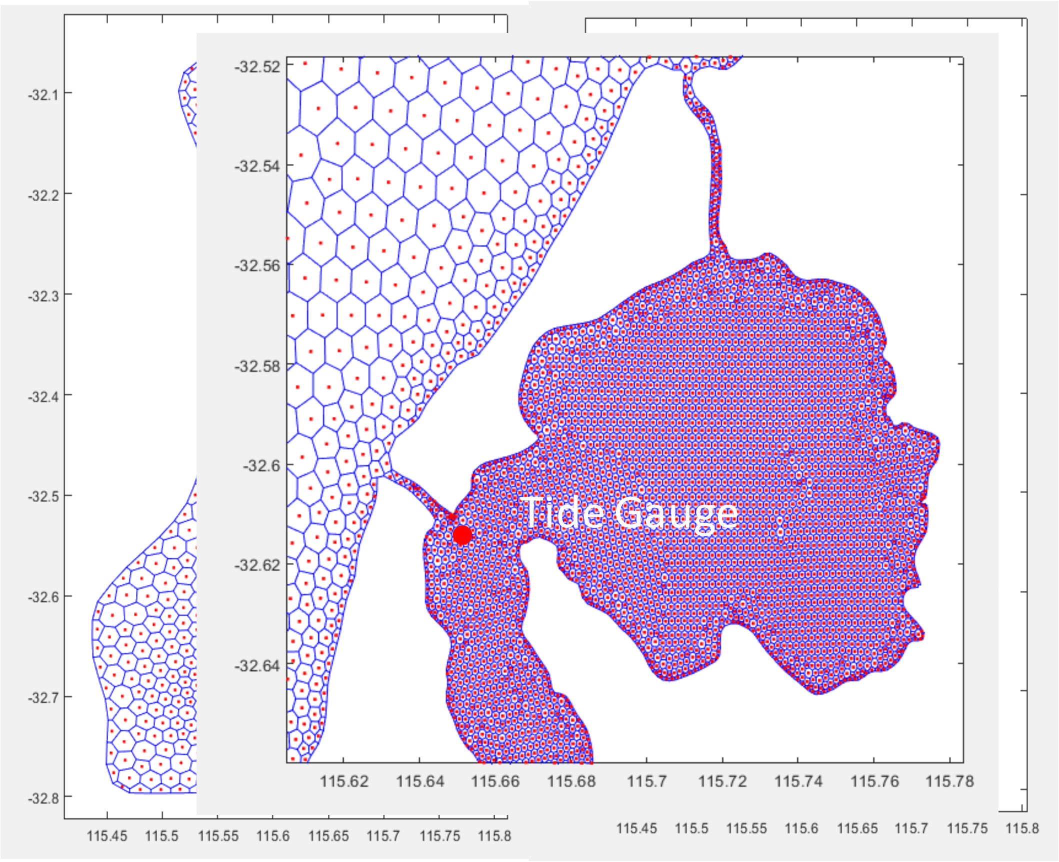

Mandurah, WA Test Bed - June 2019

- Surface Elevation (η)

Hs

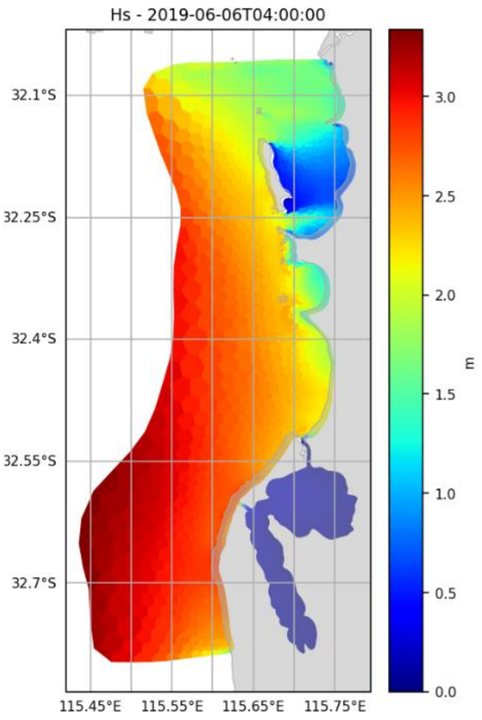

Hydro only

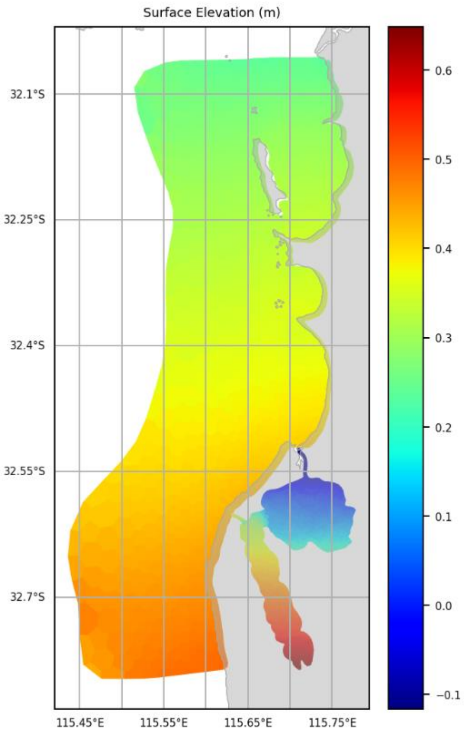

Hydro + Waves

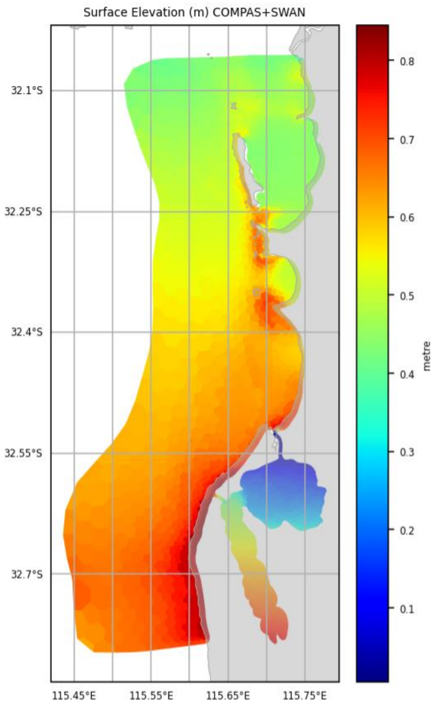

Waves- Hydro

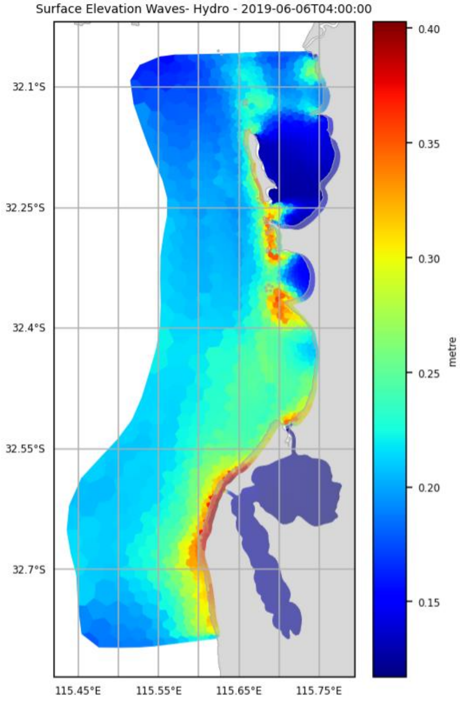

Mandurah, WA Test Bed - June 2019

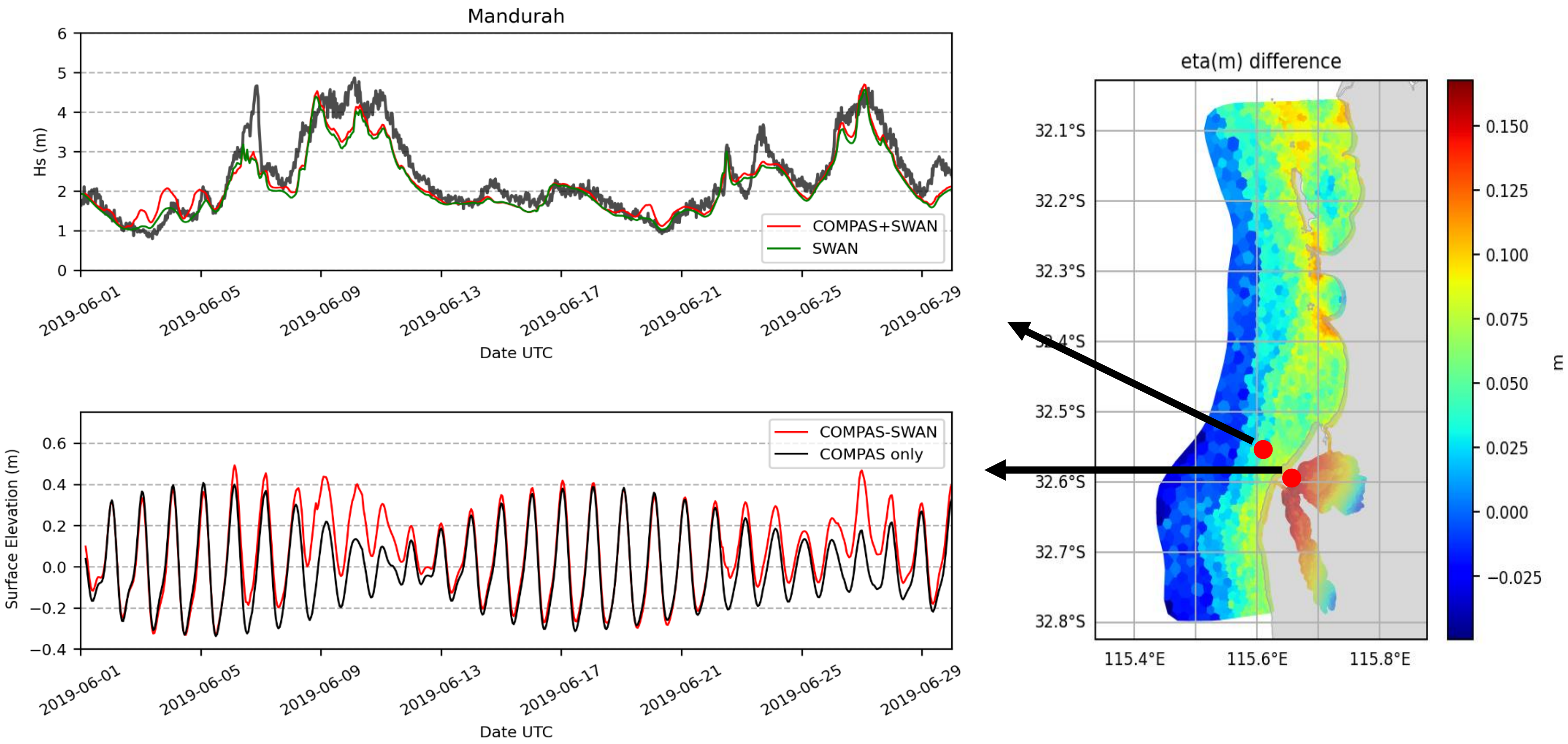

Mandurah, WA Test Bed - June 2019

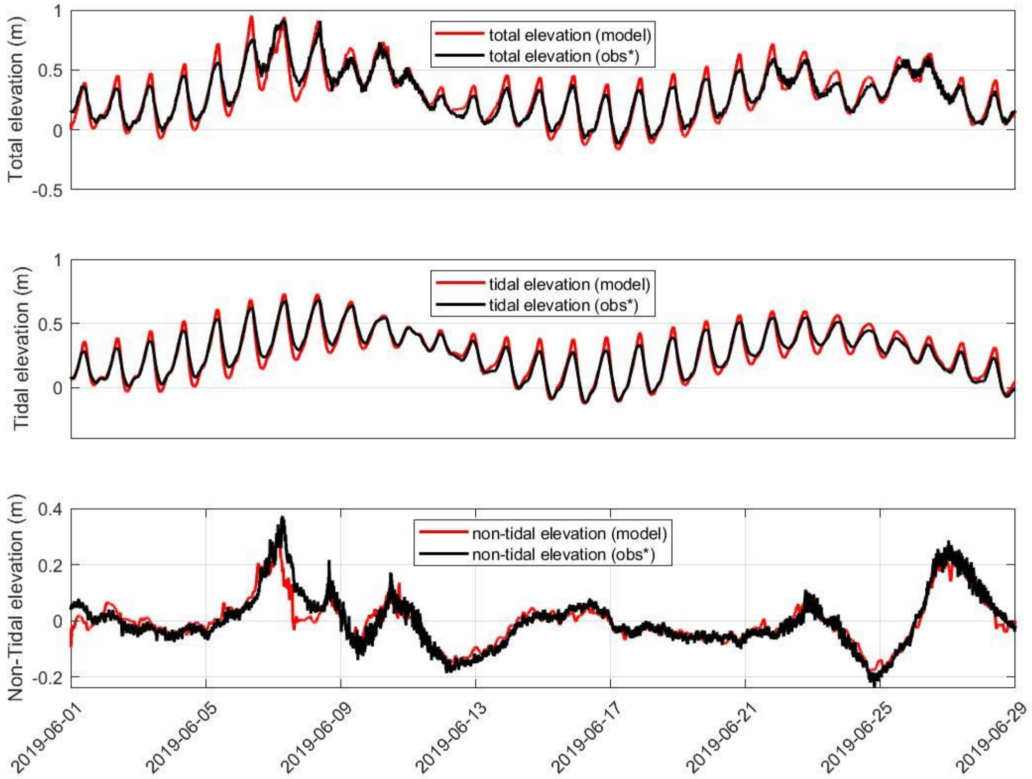

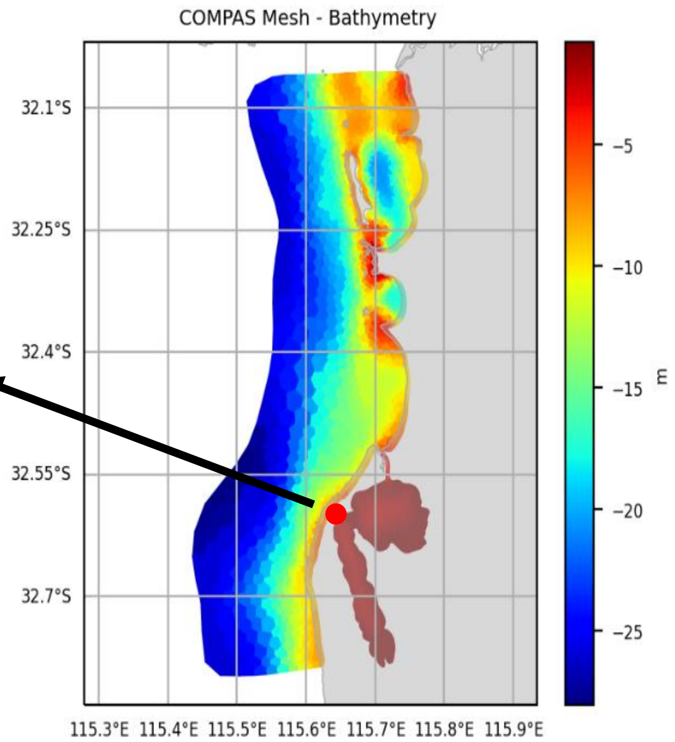

Mandurah, WA Test Bed - June 2019

Rottnest Island

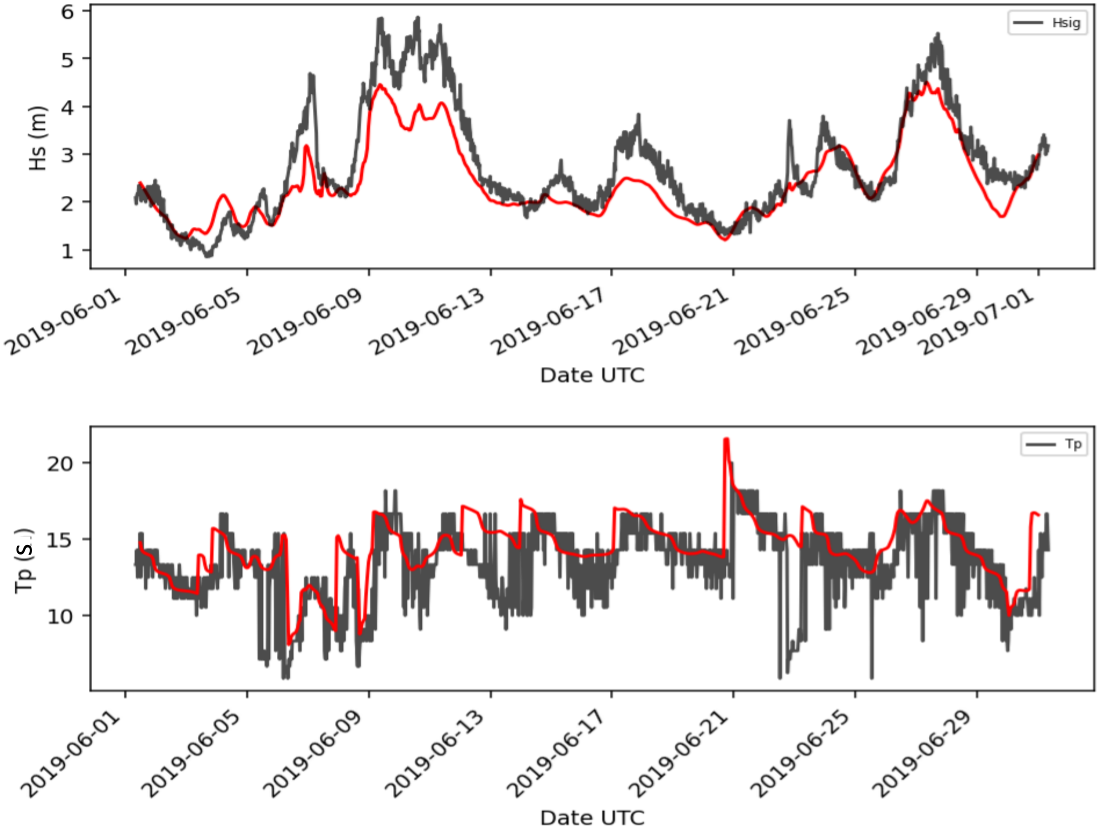

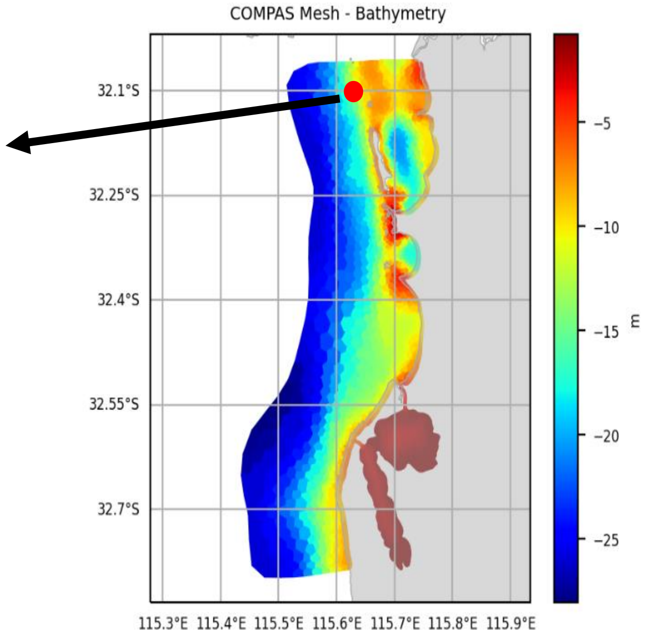

Mandurah - August-Sep 21

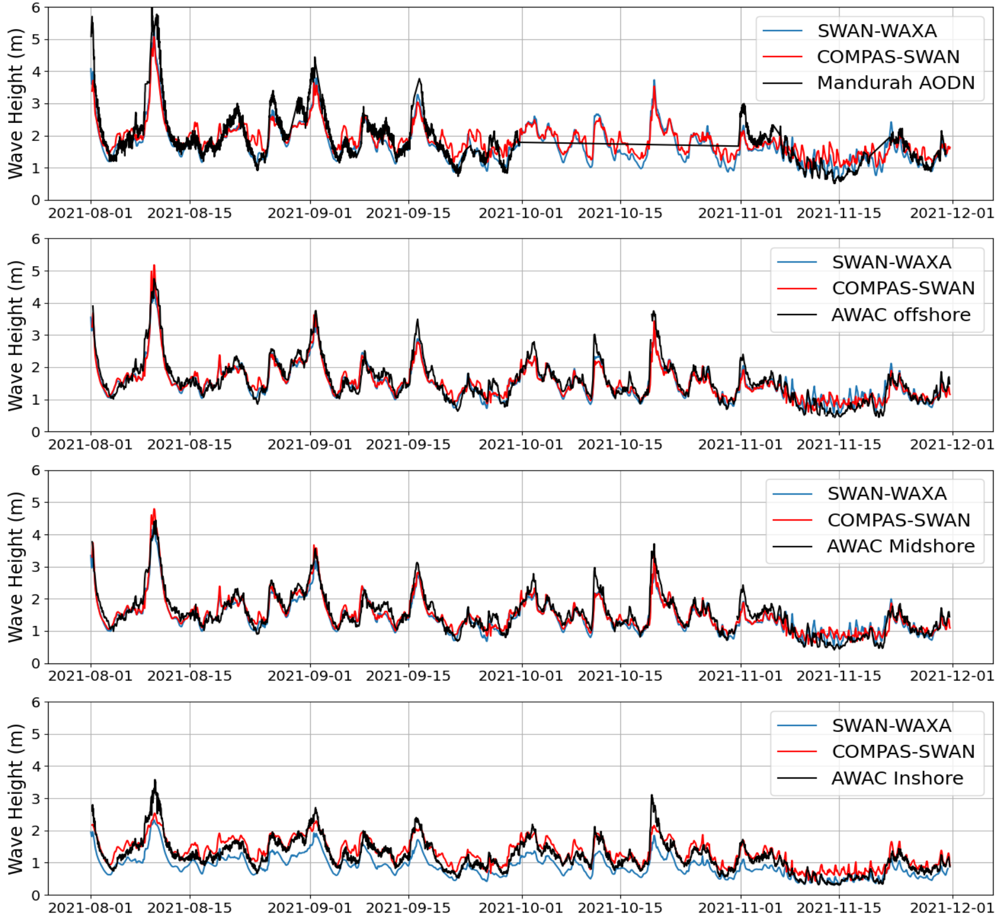

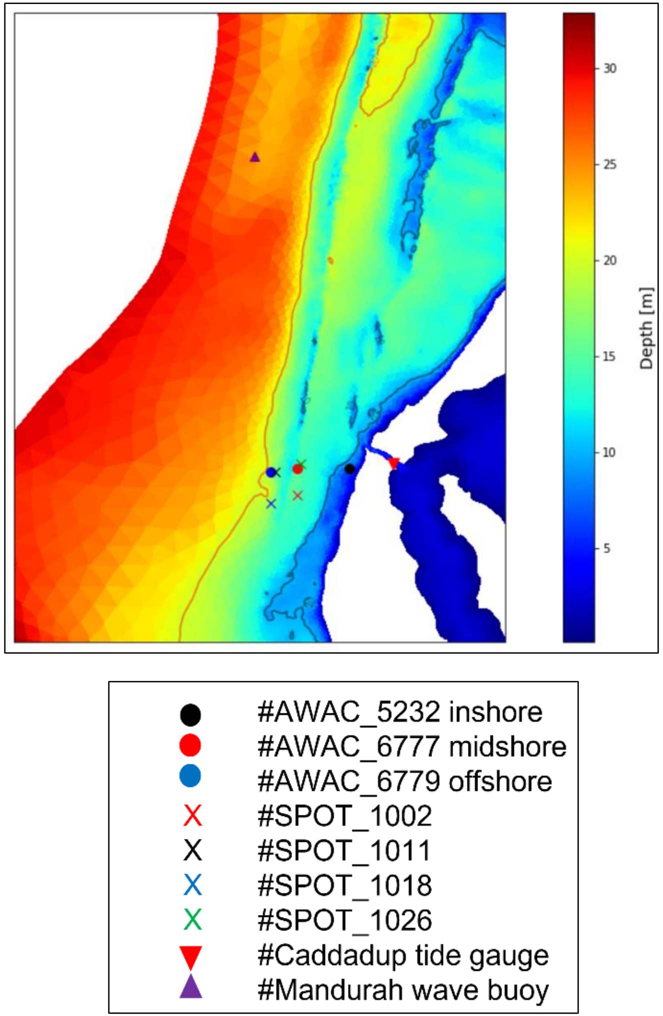

Mandurah - August-Sep 21

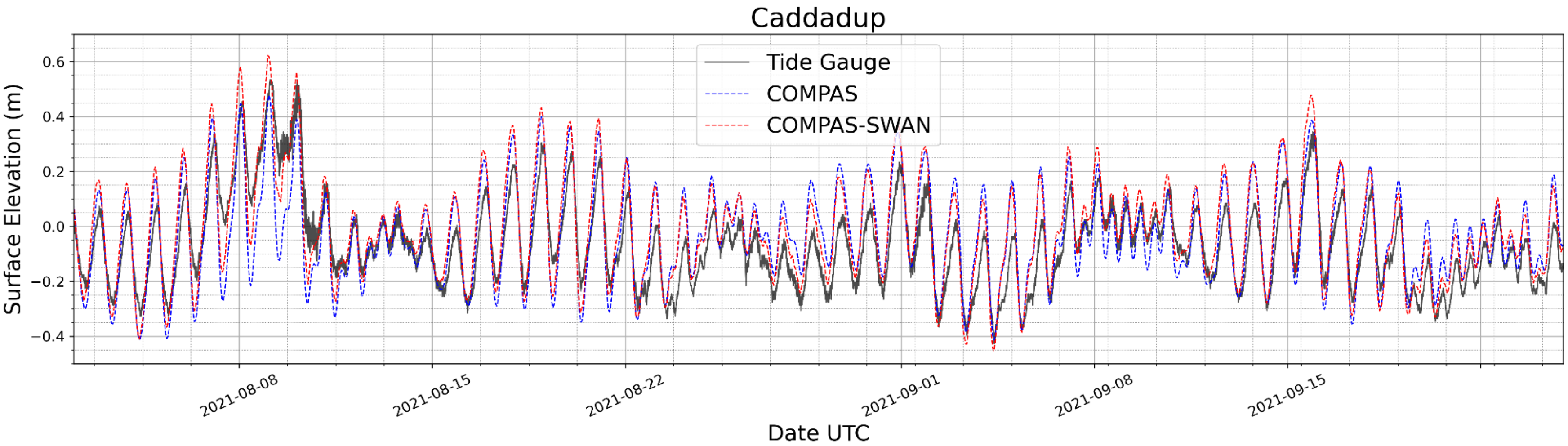

Mandurah, WA Test Bed - June 2019

- Stoke Drift and Bernoulli Head

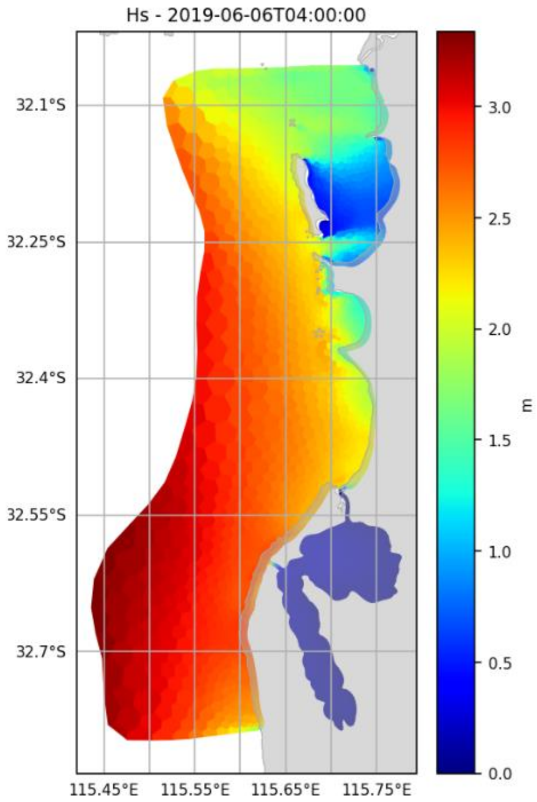

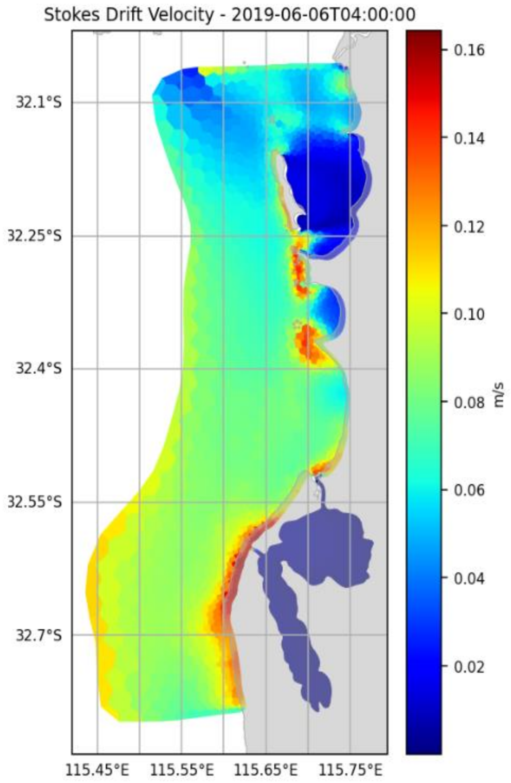

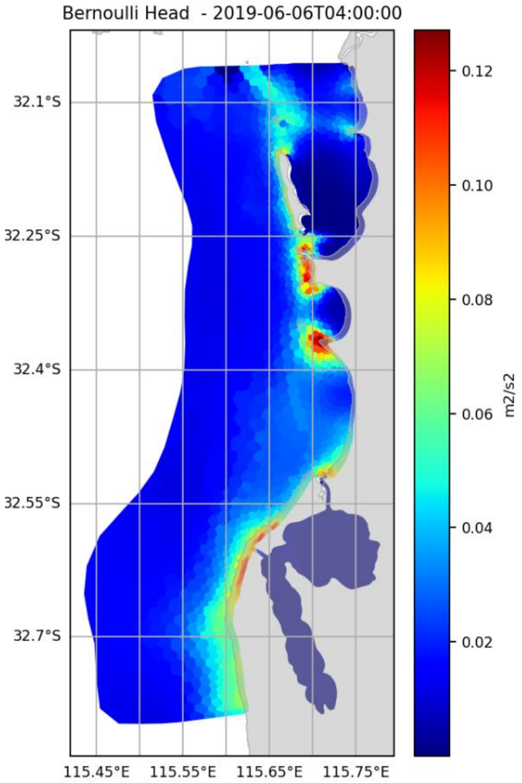

Non-conservative WEC Terms

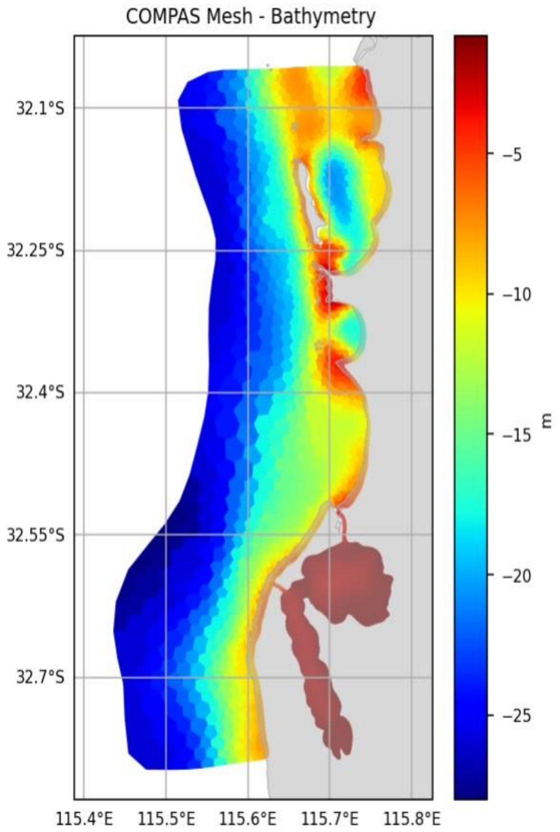

Bottom Friction

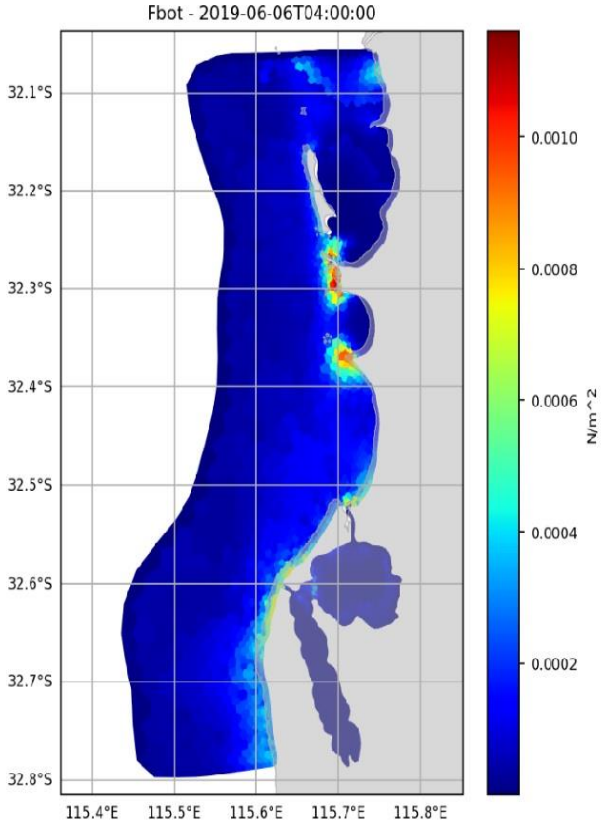

Depth Induced Breaking

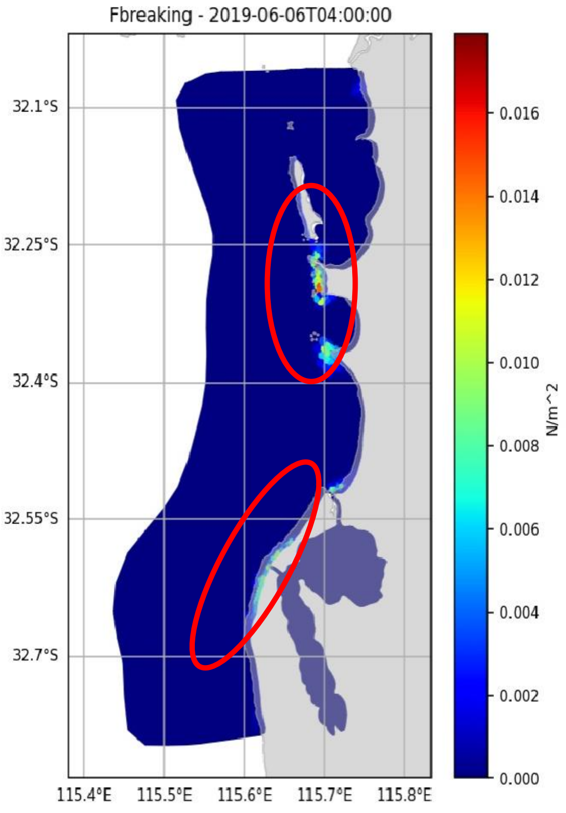

Mandurah, WA Test Bed - August 2021

Depth Induced Breaking

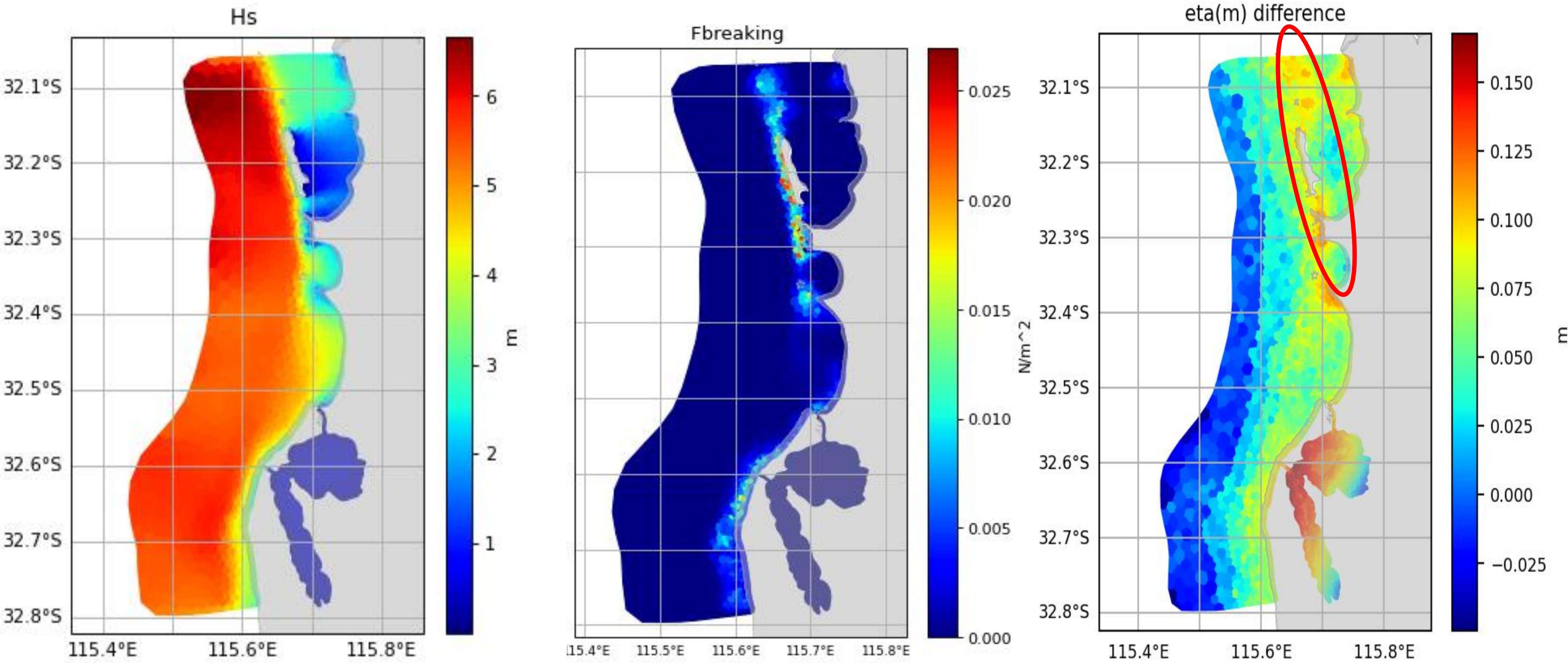

Non-conservative WEC Terms

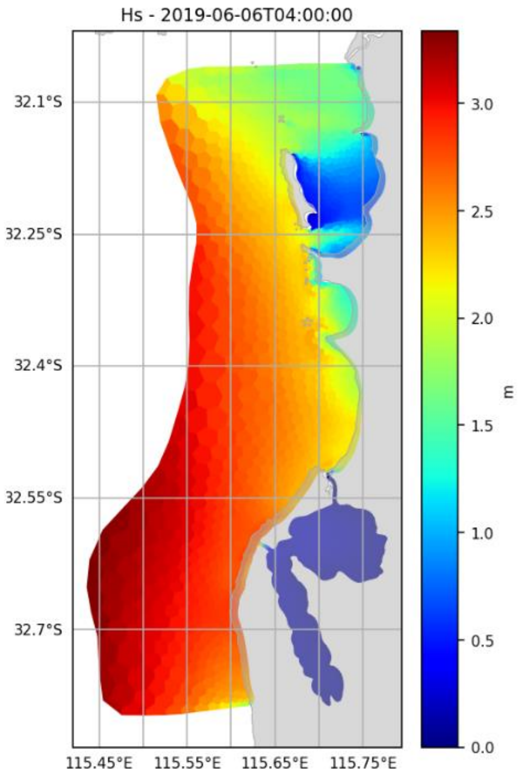

Whitecapping

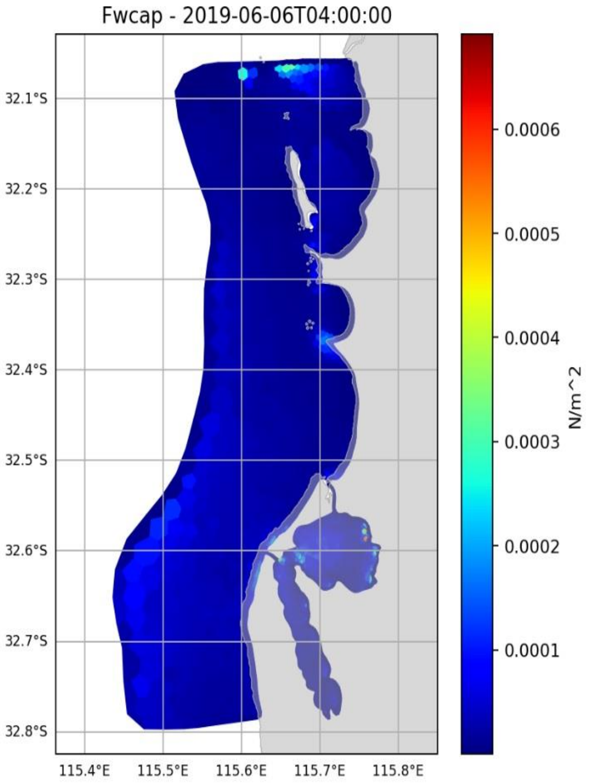

Surface Streaming

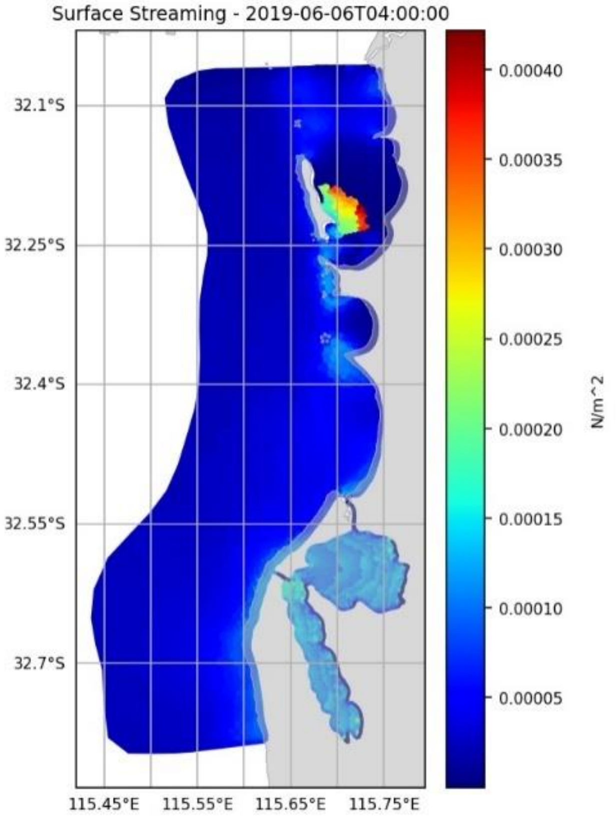

Summary and Future Work

- COMPAS-SWAN coupled model available https://github.com/csiro-coasts/EMS

COMPAS
Coastal Ocean Marine Prediction Across Scales

- Vortex-Force Formalization between COMPAS-SWAN
- Unstructured mesh generation capability
- Impact of depth-induced wave breaking on surface elevation

- ***Ongoing and Future Work***
- Roller Energy Density (Reniers, 2004)
- Cyclic boundary forcing
- Scalability

Thank you

Cagil Kirezci
Cagil.Kirezci@csiro.au

References

- Engwirda, D., 2017. JIGSAW(GEO) 1.0: locally-orthogonal staggered unstructured grid generation for general circulation modelling on the sphere. Geosci. Model Dev 10 (6), 2117.
- Herzfeld, M., Engwirda, D., & Rizwi, F. (2020). A coastal unstructured model using Voronoi meshes and C-grid staggering. Ocean Modelling, 148, 101599.
- Herzfeld, M., 2006. An alternative coordinate system for solving finite difference ocean models. Ocean Model. 14 (3–4), 174–196.
- Kumar, N., Voulgaris, G., Warner, J. C., & Olabarrieta, M. (2012). Implementation of the vortex force formalism in the coupled ocean-atmosphere-wave-sediment transport (COAWST) modeling system for inner shelf and surf zone applications. Ocean Modelling, 47, 65-95.
- Reniers, A. J., Roelvink, J. A., & Thornton, E. B. (2004). Morphodynamic modeling of an embayed beach under wave group forcing. Journal of Geophysical Research: Oceans, 109(C1).
- Ringler, T., Petersen, M., Higdon, R. L., Jacobsen, D., Jones, P. W., & Maltrud, M. (2013). A multi-resolution approach to global ocean modeling. Ocean Modelling, 69, 211-232.
- Romero, L., Hypolite, D., & McWilliams, J. C. (2021). Representing wave effects on currents. Ocean Modelling, 167, 101873.
- Svendsen, I. A. (1984). Wave heights and set-up in a surf zone. Coastal engineering, 8(4), 303-329.
- Uchiyama, Yusuke, James C. McWilliams, and Alexander F. Shchepetkin. "Wave–current interaction in an oceanic circulation model with a vortex-force formalism: Application to the surf zone." Ocean Modelling 34.1-2 (2010): 16-35.
- Zijlema, M. (2010). Computation of wind-wave spectra in coastal waters with SWAN on unstructured grids. Coastal Engineering, 57(3), 267-277.

Summary and Future Work

- COMPAS-SWAN coupled model available
  https://github.com/csiro-coasts/EMS

COMPAS

Coastal Ocean Marine Prediction Across Scales

- Vortex-Force Formalization between COMPAS-SWAN
- Unstructured mesh generation capability
- Impact of depth-induced wave breaking on surface elevation

- ***Ongoing and Future Work***
- Roller Energy Density (Reniers, 2004)
- Cyclic boundary forcing
- Scalability

Wave Roller Dissipation

- Wave rollers act as storage of dissipated wave energy, which is gradually transferred to the mean flow causing a lag in the transfer of momentum

- Depth – Induced Wave Breaking $\mathbf{B}^b = \frac{(1-\alpha^r)\epsilon^b}{\rho_0 \sigma}\mathbf{k} \cdot f^b(z)$

- Wave Roller Contribution $\mathbf{B}^r = \frac{\epsilon^r}{\rho_0 \sigma}\mathbf{k} \cdot f^b(z)$ $\qquad \varepsilon^r = \frac{g \cdot \sin\beta \cdot E^r}{c}$

- Wave Roller Model of Svendsen (1984) ➔applied

- Using Roller Energy Density (Reniers, 2004) → application in progress $\frac{\partial \mathcal{A}^r}{\partial t} + \nabla \cdot (\mathcal{A}^r \mathbf{c}) = \frac{\alpha_r \varepsilon^b - \varepsilon^r}{\sigma}$

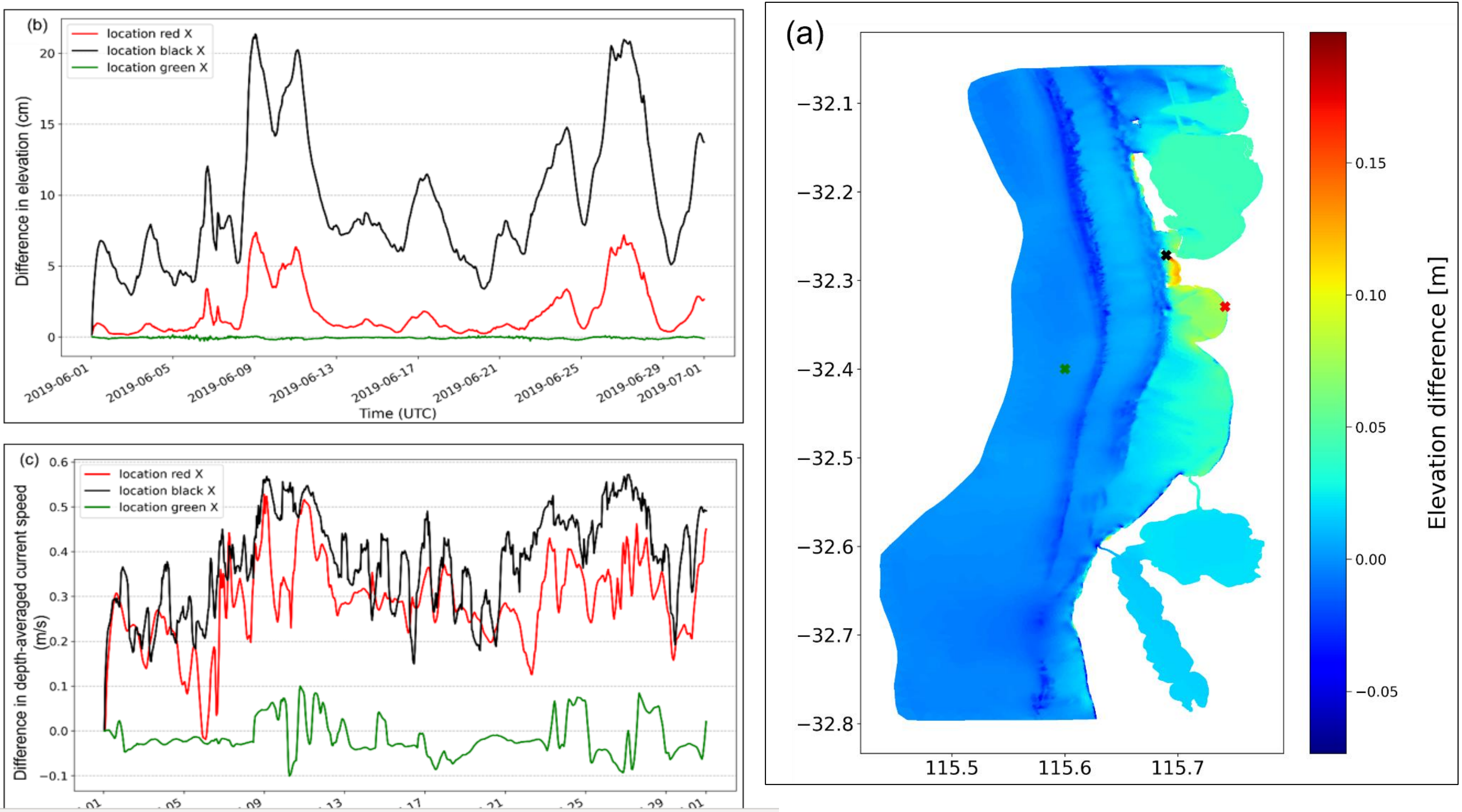
(b)
location red X
location black X
location green X
Difference in elevation (cm)
20
15
10
5
0
2019-06-01
2019-06-05
2019-06-09
2019-06-13
2019-06-17
2019-06-21
2019-06-25
2019-06-29
2019-07-01
Time (UTC)
(c)
location red X
location black X
location green X
Difference in depth-averaged current speed (m/s)
0.6
0.5
0.4
0.3
0.2
0.1
0.0
−0.1
(a)
−32.1
−32.2
−32.3
−32.4
−32.5
−32.6
−32.7
−32.8
115.5
115.6
115.7
Elevation difference [m]
0.15
0.10
0.05
0.00
−0.05